NASA CR-165,776

NASA Contractor Report 165776

NASA-CR-165776

1981 0024957

THE CRACK PROBLEM FOR A HALF PLANE
STIFFENED BY ELASTIC COVER PLATES

F. Delale and F. Erdogan

LEHIGH UNIVERSITY
Bethlehem, Pennsylvania   18015

NASA

National Aeronautics and
Space Administration

Langley Research Center
Hampton, Virginia 23665

THE CRACK PROBLEM FOR A HALF PLANE
STIFFENED BY ELASTIC COVER PLATES*

by

F. Delale and F. Erdogan
Lehigh University, Bethlehem, PA 18015

ABSTRACT

In this paper the problem of an elastic half plane containing a crack and stiffened by a cover plate is considered. First, the asymptotic nature of the stress state in the half plane around an end point of the stiffener is studied in order to determine the likely orientation of a possible fracture initiation and growth. The problem is then formulated for an arbitrary oriented radial crack in terms of a system of singular integral equations. For an internal crack and for an edge crack, the problem is solved and the stress intensity factors at the crack tips and the interface stress are calculated. The case of a cracked half plane for two symmetrically located cover plates is then considered. From a fracture viewpoint, the case of two stiffeners appears to be more severe than that of a single stiffener.

1. Introduction

In the relatively recent past, there has been considerable interest in the analysis of "cover plates" as a problem in structural mechanics. This is primarily due to the fact that the structural components with a variety of bonded or welded stiffeners and the solid state devices containing elastic wafers fuse-bonded to elastic substrates may be approximated by a cover plate bonded to an elastic solid. In most cases, since the stiffener is relatively very thin compared to the remaining dimensions of the structure, it is approximated by an elastic "membrane" neglecting the normal stress along the interface. Typical examples for such studies may be found in [1-3]. The primary interest in these and similar studies has been in the evaluation of the contact shear along the interface. The

---

results given in [3] for various elastic and inextensible cover plate geometries show that, at the end points of the stiffener, not only the contact shear stress but also the stress state in the substrate has a $r^{-1/2}$ singularity. This suggests that such points of stress singularity are locations of potential failure initiation. Furthermore, if the bond is sufficiently strong, the most likely failure mechanism would be the initiation and propagation of a crack in the substrate along the weakest cleavage plane emanating from the singular point. To study the related failure problem, one needs to determine the weakest cleavage plane in the elastic half plane and to solve the corresponding crack problem by placing a crack of arbitrary length along this plane.

A problem similar to that described above was considered in a recent paper [4], where it was assumed that the stiffener is perfectly rigid and the crack is perpendicular to the boundary. Aside from the assumption regarding the stiffness of the cover plate which may not be very realistic for most practical applications, in [4] it is found that the nature of the stress singularities at both ends of the cover plate are identical to that of stiffened uncracked elastic half plane where the power of singularity is complex. This is clearly incorrect as the zero traction-zero displacement mixed boundary conditions which prevails in the half plane near the end points are for a wedge of angle π at one end and $\pi/2$ at the other[*]. At the crack end of the stiffener, that is, for the 90-degree wedge, the power of the singularity is less than one half and is real [5].

The general formulation given in this paper may be used to reduce a number of crack-stiffener or crack-contact problems (including that discussed in [4]) to a system of integral equations. Since the kernels in these integral equations are known in closed form and are relatively simple functions, quite accurate solutions to the problem may be obtained with a minimal computational effort.

---

[*] This is due to "rounding" the corners by approximating the mapping function by a rational function used in [4] for mapping the cracked half plane into a circle.

2. Formulation of the Problem

The problem under consideration is that of an elastic half plane $(-\infty < x < \infty, y < 0)$ which contains an arbitrarily oriented crack and is subjected to a given set of external loads. Along the boundary $y = 0$ the plane may contain a bonded stiffener or may be loaded through a stamp. Perhaps the simplest way to solve the problem would be to reduce it to a system of integral equations in which the crack surface displacements and the contact stresses on the boundary are the unknown functions. To derive the integral equations, in addition to the solution of the problem for the half plane under the given applied loads but without the crack and the stiffener, it is sufficient to obtain the solution for a dislocation in the plane and a concentrated force on the boundary.

Consider a half plane $(-\infty < x < \infty, -\infty < y < 0)$ with the elastic constants κ_2, μ_2 ($\kappa_2 = 3 - 4\nu_2$ for plane strain and $\kappa_2 = (3-\nu_2)/(1+\nu_2)$ for plane stress) which contains a dislocation at the point (x_1, y_1) having a Burger's vector $\vec{b}$. Let the components of the Burger's vector be $b_x = f_1$ and $b_y = f_2$. Referring to [6] the stress state in the half plane due to f_1 and f_2 may be expressed as

$$\sigma_{1xx}(x,y) = \frac{2\mu_2}{\pi(1+\kappa_2)} [K_{11}(x,y,x_1,y_1)f_1 + K_{12}(x,y,x_1,y_1)f_2],$$

$$\sigma_{1xy}(x,y) = \frac{2\mu_2}{\pi(1+\kappa_2)} [K_{21}(x,y,x_1,y_1)f_1 + K_{22}(x,y,x_1,y_1)f_2],$$

$$\sigma_{1yy}(x,y) = \frac{2\mu_2}{\pi(1+\kappa_2)} [K_{31}(x,y,x_1,y_1)f_1 + K_{32}(x,y,x_1,y_1)f_2].$$

$$(1.a-c)$$

where the functions K_{ij} are given in Appendix A.

The second basic solution needed to formulate the problem is that of a half plane under concentrated forces f_3 and f_4 acting on the boundary at $(x = x_0, y=0)$ in x and y directions, respectively. This solution is

given by

$$\sigma_{2xx}(x,y) = -\frac{2}{\pi r^4} [(x-x_0)^3 f_3 + (x-x_0)^2 y\, f_4],$$

$$\sigma_{2xy}(x,y) = -\frac{2}{\pi r^4} [(x-x_0)^2 y\, f_3 + (x-x_0)y^2\, f_4],$$

$$\sigma_{2yy}(x,y) = -\frac{2}{\pi r^4} [y^2(x-x_0)f_3 + y^3 f_4], \tag{2a-c}$$

where

$$r^2 = (x-x_0)^2 + y^2 . \tag{3}$$

For this loading condition, the displacement derivatives on the boundary $y=0$ may be expressed as

$$\frac{4\mu_2}{1+\kappa_2} \frac{\partial}{\partial x} u_2(x,0) = \frac{1}{\pi} \frac{f_3}{x_0-x} + \frac{\kappa_2-1}{\kappa_2+1} f_4\, \delta(x-x_0) ,$$

$$\frac{4\mu_2}{1+\kappa_2} \frac{\partial}{\partial x} v_2(x,0) = -\frac{\kappa_2-1}{\kappa_2+1} f_3\, \delta(x-x_0) + \frac{1}{\pi} \frac{f_4}{x_0-x} . \tag{4a,b}$$

The third problem is the determination of the stress state in the half plane having no crack and no stiffener and subjected to the actual applied loads. This stress state will be designated by $\sigma_{aij}(x,y)$, $(i,j = x,y)$. For example, in a plane under uniform tension p_0 in x-direction, we have

$$\sigma_{axx}(x,y) = p_0, \quad \sigma_{axy}(x,y) = 0, \quad \sigma_{ayy}(x,y) = 0. \tag{5a-c}$$

Consider now the problem described in Figure 1. If the cover plate is approximated by a membrane, $\sigma_{yy} = 0$ and the equilibrium condition in x-direction gives

$$\frac{8\mu_1}{1+\kappa_1} \frac{\partial u_1}{\partial x} h = \int_{-2a}^{x} f_3(x_0)dx_0 + P_1 \tag{6}$$

where μ_1 and κ_1 are the elastic constants, h the thickness, u_1 the displacement, 2a the length of the stiffener, P_1 and P_2 the additional forces which may be acting on the stiffener, and $f_3(x_0) = \sigma_{xy}$ the shear stress acting on the contact region (Figure 1). Note that

$$\int_{-2a}^{0} f_3(x_0)dx_0 = P_2 - P_1 . \tag{7}$$

If we now assume that the half plane contains a crack along the line L, the Burger's vector $\vec{b}(f_1,f_2)$ would be a continuously distributed function with the coordinates x_1 and y_1 on L. Clearly, $f_1(x_1,y_1)$, $f_2(x_1,y_1)$ and $f_3(x_0)$ are the unknown functions of the problem which may be determined from the traction boundary conditions on the crack surface and the displacement continuity along the contact area. Anticipating the crack initiation at an end region of the stiffener, consider the specific radial crack geometry shown in Figure 1. The boundary conditions on the crack surface may be expressed as

$$\sigma_{nn}(s) = \sigma_{xx}\cos^2\theta + \sigma_{yy}\sin^2\theta + \sigma_{xy}\sin2\theta = 0, \quad c < s < d,$$

$$\sigma_{sn}(s) = (\sigma_{xx}-\sigma_{yy})\sin\theta \cos\theta - \sigma_{xy}\cos2\theta = 0, \quad c < s < d, \tag{8a,b}$$

where (see (1), (2) and (5))

$$\sigma_{ij} = \sigma_{1ij} + \sigma_{2ij} + \sigma_{aij}, \quad (i,j) = (x,y). \tag{9}$$

On the line of the crack note that

$$x = s \sin\theta , \quad y = -s \cos\theta , \tag{10}$$

and we let

$$x_1 = t \sin\theta, \quad y_1 = -t \cos\theta, \quad (c < t < d).$$ \hfill (11)

Now, observing that f_1, f_2 and f_3 are distributed functions, substituting from (1), (2), (5), and (9-10) into (8) we obtain the following two integral equations:

$$\int_c^d k_{11}(s,t)f_1(t)dt + \int_c^d k_{12}(s,t)f_2(t)dt + \int_{-2a}^0 k_{13}(s,x_0)f_3(x_0)dx_0$$

$$= - p_0 \cos^2\theta, \quad (c < s < d),$$

$$\int_c^d k_{21}(s,t)f_1(t)dt + \int_c^d k_{22}(s,t)f_2(t)dt + \int_{-2a}^0 k_{23}(s,x_0)f_3(x_0)dx_0$$

$$= - p_0 \sin\theta \cos\theta, \quad (c < s < d) ,$$ \hfill (12a,b)

where the kernels k_{ij}, ($i=1,2$; $j=1,2,3$) are given in Appendix B. Since the crack is an embedded crack, from the condition of single-valuedness of displacements it follows that

$$\int_c^d f_1(t)dt = 0 , \quad \int_c^d f_2(t)dt = 0 .$$ \hfill (13a,b)

The third integral equation is obtained by expressing the condition of continuity of $\partial u/\partial x$ along the interface $y=0$, $-2a < x < 0$, namely

$$\frac{\partial}{\partial x} u_1(x) = \frac{\partial}{\partial x} u_2(x,0).$$ \hfill (14)

The strain $\partial u_1/\partial x$ is given by (6). $\partial u_2/\partial x$ is obtained by adding the strains given by the stress states (1), (2) (which is given by (4a)),

and (5), and again keeping in mind that f_1, f_2, and f_3 are distributed functions. Thus, for the crack geometry and the applied loads given in Figure 1 we obtain

$$\int_c^d k_{31}(x,t)f_1(t)dt + \int_c^d k_{32}(x,t)f_2(t)dt + \int_{-2a}^0 k_{33}(x,x_0)f_3(x_0)dx_0$$

$$= -\frac{1+\kappa_2}{8\mu_2} P_0 + \frac{1+\kappa_1}{8h\mu_1} P_1 \ , \ (-2a < x < 0), \tag{15}$$

where the kernels k_{3j}, $(j=1,2,3)$ are also given in Appendix B.

3. The Uncracked Plane

To determine the direction of crack initiation in the plane, the asymptotic stress state near the end points of the stiffener needs to be analyzed. In the uncracked plane, the external loads are the actual applied loads (e.g., $\sigma_{xx}(\infty,y) = p_0$) and the contact stresses on the stiffener-half plane interface. If the stiffener is approximated by a membrane, the contact stress $\sigma_{yy}(x,0) = f_4(x)$ is zero and referring to the insert in Figure 2, for $P_1=P_2=0$, $\sigma_{xy}(x,0) = f_3(x)$ is determined from (see (15))

$$\frac{1}{\pi}\int_0^b \frac{f_3(x_0)}{x_0-x} dx_0 - \frac{1}{2h}\frac{\mu_2(1+\kappa_1)}{\mu_1(1+\kappa_2)}\int_0^x f_3(x_0)dx_0 = -p_0/2, \ (0 < x < b),$$

$$\tag{16}$$

subject to

$$\int_0^b f_3(x_0)dx_0 = 0 \ . \tag{17}$$

Defining

$$x = (1+t)b/2, \quad x_0 = (1+\tau)b/2, \quad f_3(x_0) = f(\tau), \quad \lambda = \frac{b\mu_2(1+\kappa_1)}{h\mu_1(1+\kappa_2)}, \quad (18)$$

equations (16) and (17) may be expressed as

$$\frac{1}{\pi} \int_{-1}^{1} \frac{f(\tau)}{\tau-t}\, d\tau - \frac{\lambda}{4} \int_{-1}^{t} f(\tau)d\tau = -p_0/2, \quad (-1 < t < 1),$$

$$\int_{-1}^{1} f(\tau)d\tau = 0 \qquad\qquad (19a,b)$$

which are solved numerically.

Once $f_3(x_0)$ is determined, by substituting from (2) into the transformation formulas (8) and integrating in x_0, one may easily obtain the cleavage stress σ_{nn} along $n=0$ as follows:

$$\frac{1}{p_0} \sigma_{nn}(r,\theta) = -\frac{1}{\pi} \int_{-1}^{1} \{[r\sin\theta + (1-\tau)/2]^3 \cos^2\theta + [r\sin\theta$$

$$+ (1-\tau)/2]r^2 \sin^2\theta \cos^2\theta - 2r[r\sin\theta$$

$$+ (1-\tau)/2]^2 \sin\theta \cos^2\theta\}\{r^2\cos^2\theta + [r\sin\theta$$

$$+ (1-\tau)/2]^2\}^{-2} f(\tau)d\tau + \cos^2\theta, \quad (0 < r < \infty), \qquad (20)$$

where $r = s/b$. Also, on the boundary $y=0$ the stress component σ_{xx} may be obtained from (2a) as follows:

$$\frac{1}{p_0} \sigma_{xx}(x,0) = 1 + \frac{2}{\pi} \int_{-1}^{1} \frac{f(\tau)}{\tau-t}\, d\tau, \quad x = b(t+1)/2, \quad (-\infty < t < \infty). \quad (21)$$

Note that the solution of (19a) is of the form

$$f(\tau) = F(\tau)/(1-\tau^2)^{1/2} \quad (-1 < \tau < 1), \tag{22}$$

$F(\tau)$ being a bounded function. Thus, after determining $F(\tau)$ from (19), $\sigma_{nn}(r,\theta)$ and $\sigma_{xx}(x,0)$ may be obtained from (20) and (21) by using the standard Gaussian integration formulas [7]. Figure 2 shows the variation of the cleavage stress σ_{nn} with the angle θ for a fixed value of $r=s/b$. The value of r seems to affect primarily the magnitude rather than the angular variation of σ_{nn}. The angle at which σ_{nn} is maximum is approximately 3 degrees. By changing λ it was also observed that this angle does not seem to vary significantly with material constants. Therefore, for the remainder of this study, it will be assumed that the weak cleavage plane in the elastic half space is $\theta \cong 0$. This way the integral equations and the subsequent asymptotic analysis are simplified quite considerably without significantly altering the qualitative behavior of the results. Along the plane $\theta = 0$, the variation of the cleavage stress $\sigma_{nn}(s,0) = \sigma_{xx}(b,y)$ is shown in Figure 3. From (20) it can be shown that σ_{nn} has a singularity of the form $s^{-1/2}$ in the neighborhood of the end points of the stiffener. Thus, σ_{nn} becomes unbounded as $s \to 0$.

By substituting from (22) into (21) and by using the properties of the Cauchy-type integrals or that of the Chebishev polynomials, it may easily be shown that [7] the function $\sigma_{xx}(x,0)$ defined by (21) is bounded in $-1 < t < 1$, (or in $0 < x < b$) and has a square-root singularity at $t = \mp 1$ (or at $x=0$, $x=b$) for $|t| > 1$. That is, as may be seen from Figure 4, $\sigma_{xx}(x,0)$ is discontinuous and is unbounded at the end points of the stiffener.

4. The Crack-Stiffener Problem-The Internal Crack

For uniform tension p_0, $P_1 = P_2 = 0$, and $\theta = 0$ from (12) and (15) the integral equations of the problem shown in Figure 1 may be obtained as follows:

$$\frac{2\mu_2}{\pi(1+\kappa_2)} \int_c^d [- \frac{1}{t-s} - \frac{1}{t+s} - \frac{2t}{(t+s)^2} + \frac{4t^2}{(t+s)^3}] f_1(t)dt$$

$$+ \frac{2}{\pi} \int_{-2a}^0 \frac{x_0^3 f_3(x_0)dx_0}{(x_0^2+s^2)^2} = -p_0, \quad (c < s < d) , \qquad (23)$$

$$\frac{2\mu_2}{\pi(1+\kappa_2)} \int_c^d [\frac{1}{t-s} + \frac{s^2-t^2+4ts}{(t+s)^3}] f_2(t)dt - \frac{2}{\pi} \int_{-2a}^0 \frac{sx_0^2 f_3(x_0)dx_0}{(x_0^2+s^2)^2} = 0 ,$$

$$(c < s < d) , \qquad (24)$$

$$\frac{1}{2\pi} \int_c^d [\frac{-t}{t^2+x^2} + \frac{t(t^2-3x^2)}{(t^2+x^2)^2}] f_1(t)dt - \frac{2}{\pi} \int_c^d \frac{t^2 x}{(t^2+x^2)^2} f_2(t)dt$$

$$+ \frac{1+\kappa_2}{4\pi\mu_2} \int_{-2a}^0 \frac{f_3(x_0)}{x_0-x} dx_0 - \frac{1+\kappa_1}{8h\mu_1} \int_{-2a}^x f_3(x_0)dx_0 = - \frac{1+\kappa_2}{8\mu_2} p_0 ,$$

$$(-2a < x < 0) , \qquad (25)$$

The solution of (23-25) is to be obtained under the following conditions:

$$\int_c^d f_1(t)dt = 0, \quad \int_c^d f_2(t)dt = 0, \quad \int_{-2a}^0 f_3(x_0)dx_0 = 0 . \qquad (26a\text{-}c)$$

For c>0 the integral equations (23-25) have simple Cauchy-type kernels. Consequently, the functions f_i, (i=1,2,3) have square root singularities and are of the form shown by (22). These equations may

easily be solved by using a Gaussian quadrature formula [7]. From the viewpoint of fracture analysis, the quantities which are of primary interest are the stress intensity factors which may be obtained as follows[*]:

$$k_1(c) = \lim_{s \to c} \sqrt{2(c-s)}\sigma_{xx}(s,0), \quad k_2(c) = \lim_{s \to c} \sqrt{2(c-s)}\sigma_{xy}(s,0) , \qquad (27a,b)$$

$$k_1(d) = \lim_{s \to d} \sqrt{2(s-d)}\sigma_{xx}(s,0), \quad k_2(d) = \lim_{s \to d} \sqrt{2(s-d)}\sigma_{xy}(s,0), \qquad (28a,b)$$

$$k_2(-2a) = \lim_{x \to -2a} \sqrt{2(2a+x)}\sigma_{xy}(x,0), \quad k_2(0) = \lim_{x \to 0-} \sqrt{-2x}\sigma_{xy}(x,0). \qquad (29a,b)$$

5. The Edge Crack

The integral equations (23-25) are valid for all cracks perpendicular to the boundary, including the physically important case of an edge crack for which c=0. It may be observed that for c=0 the kernels of the integral equations are of the generalized Cauchy type; that is, in addition to simple Cauchy singularities, the kernels contain terms which become unbounded at the end point x=0=s. Consequently, at the end point x=0=s the functions f_i, (i=1,2,3) would not have the standard square-root singularity.

First, we note that for a sectionally holomorphic function F(z) defined by

---

[*]Note that for the geometry under consideration

$$f_1(y) = \frac{\partial}{\partial y}[u_2(+0,y)-u_2(-0,y)] \text{ and } f_2(y) = \frac{\partial}{\partial y}[v_2(+0,y)-v_2(-0,y)],$$

s=-y, $\sigma_{ns}=-\sigma_{xy}$, and in transforming the coordinates the notation $f_i(s) = f_i[y(s)]$, (i=1,2) is used.

$$F(z) = \frac{1}{\pi} \int_a^b \frac{f(t)dt}{t-z} \qquad (30)$$

where

$$f(t) = \frac{\phi(t)}{(t-a)^\alpha (b-t)^\beta} , \quad (-1 < Re(\alpha,\beta) < 1), \qquad (31)$$

one may express the following asymptotic relation [7,8]:

$$F(z) = \frac{\phi(a)}{(b-a)^\beta} \frac{e^{i\alpha\pi}}{\sin\alpha\pi} \frac{1}{(z-a)^\alpha} - \frac{\phi(b)}{(b-a)^\alpha} \frac{1}{\sin\beta\pi} \frac{1}{(z-b)^\beta} + F_0(z) , \quad (32)$$

where $\phi(t)$ is a bounded function and F_0 is either bounded or has singularities of order lower than that of $F(z)$ [8]. Also note that

$$\frac{1}{\pi} \int_a^b \frac{f(t)}{(t-z)^2} dt = \frac{d}{dz} F(z) , \quad \frac{2}{\pi} \int_a^b \frac{f(t)}{(t-z)^3} dt = \frac{d^2}{dz^2} F(z) . \qquad (33)$$

By observing that for $a < x < b$ $F(z)$ is holomorphic at $z=2a-x$, one could write

$$\frac{1}{\pi} \int_a^b \frac{f(t)dt}{(t+x-2a)^{n+1}} = \frac{1}{n!} \frac{d^n}{dz^n} F(2a-x) , \quad (a < x < b). \qquad (34)$$

Thus, for c=0 the asymptotic values of all the integrals in (23-25) may be expressed in terms of the corresponding holomorphic functions by using the general relations (32) and (33) and specific expressions of the form (34). For this, it is sufficient to expand the kernels into simple fractions. For example,

$$\frac{xt^2}{(t^2+x^2)^2} = \frac{i}{4}\frac{1}{t+ix} - \frac{i}{4}\frac{1}{t-ix} + \frac{x}{4}\frac{1}{(t+ix)^2} + \frac{x}{4}\frac{1}{(t-ix)^2} , \qquad (35)$$

for which the related function $F_2(z)$ would be holomorphic at $z = \mp ix$ if $-2a < x < 0$ (see (25)).

We now let the unknown functions f_i, ($i=1,2,3$) in (23-25) be defined by

$$\frac{2\mu_2}{1+\kappa_2} f_1(t) = \frac{\phi_1(t)}{t^\beta(d-t)^\omega} , \qquad (36)$$

$$\frac{2\mu_2}{1+\kappa_2} f_2(t) = \frac{\phi_2(t)}{t^\beta(d-t)^\gamma} , \quad (0 < t < d), \qquad (37)$$

$$f_3(t) = \frac{\phi_3(t)}{(-t)^\beta(t+2a)^\alpha} , \quad (-2a < t < 0), \ 0 < \mathrm{Re}(\alpha,\beta,\gamma,\omega) < 1 . \qquad (38)$$

Also let

$$F_j(z) = \frac{2\mu_2}{1+\kappa_2}\frac{1}{\pi}\int_0^d \frac{f_j(t)}{t-z} dt, \quad (j=1,2) , \qquad (39)$$

$$F_3(z) = \frac{1}{\pi}\int_{-2a}^0 \frac{f_3(t)}{t-z} dt . \qquad (40)$$

By substituting from (36-38) into (23-25) and by using the function-theoretic method described above, the following characteristic equations may be obtained to determine the constants α, β, γ, and ω:

$$\frac{\phi_1(d)}{d^\beta} \cot\pi\omega = 0, \ -\frac{\phi_2(d)}{d^\beta} \cot\pi\gamma = 0, \ \frac{\phi_3(-2a)}{(2a)^\beta} \cot\pi\alpha = 0, \qquad (41a\text{-}c)$$

-13-

$$\frac{1}{\sin\pi\beta} \left[(1-\cos\pi\beta-4\beta+2\beta^2) \frac{\phi_1(0)}{d^\omega} + (\beta-2)\cos\frac{\pi\beta}{2} \frac{\phi_3(0)}{(2a)^\alpha} \right] = 0 , \qquad (42)$$

$$\frac{1}{\sin\pi\beta} \left[(\cos\pi\beta-1+4\beta-2\beta^2) \frac{\phi_2(0)}{d^\gamma} + (\beta-1)\sin\frac{\pi\beta}{2} \frac{\phi_3(0)}{(2a)^\alpha} \right] = 0, \qquad (43)$$

$$\frac{1}{\sin\pi\beta} \left[-2\beta\cos\frac{\pi\beta}{2} \frac{\phi_1(0)}{d^\omega} + 2(1-\beta)\sin\frac{\pi\beta}{2} \frac{\phi_2(0)}{d^\gamma} - \cos\pi\beta \frac{\phi_3(0)}{(2a)^\alpha} \right] = 0.$$
$$\qquad (44)$$

At the end points, the functions $\phi_i(t)$, (i=1,2,3) are bounded and nonzero. Hence, equations (41) give the following expected results corresponding to square-root singularities:

$$\omega = 1/2 , \quad \gamma = 1/2 , \quad \alpha = 1/2 . \qquad (45)$$

Since it is assumed that $\phi_i(0) \neq 0$, (i=1,2,3), the coefficient determinant of the linear homogeneous system (42-44) must vanish, giving the fourth characteristic equation to determine β as follows:

$$\frac{\cos\pi\beta-1}{\sin^3\pi\beta} \left[\cos\pi\beta - 1 + 4\beta - 2\beta^2\right]^2 = 0. \qquad (46)$$

It may be observed that (46) has no root for which $0 < \mathrm{Re}(\beta) < 1$. For the sectionally holomorphic function $F(z)$ given by (30), if we now assume that the density function $f(t)$ is bounded at $t=b$ and let

$$f(t) = \frac{\phi(t)}{(t-a)^{\frac{1}{2}}} , \qquad (47)$$

the asymptotic expression of $F(z)$ near the point $z=b$ becomes [8]

-14-

$$F(z) = \frac{\phi(b)}{\pi} \log (z-b) + F_0(z) , \qquad (48)$$

where, near and at $z=b$, F_0 is bounded. With the behavior at the end points known, the density functions f_i may now be expressed as

$$\frac{2\mu_2}{\kappa_2+1} f_1(t) = \frac{G_1(t)}{(d-t)^{\frac{1}{2}}} , \quad \frac{2\mu_2}{\kappa_2+1} f_2(t) = \frac{G_2(t)}{(d-t)^{\frac{1}{2}}} , \quad f_3(t) = \frac{G_3(t)}{(t+2a)^{\frac{1}{2}}} \cdot (49a\text{-}c)$$

The functions G_1 and G_2 at $t=d$ and G_3 at $t=-2a$ are bounded and nonzero. However, their behavior at $t=0$ is as yet unknown. By using (48) and substituting from (49) into the integral equations (23) and (25), we obtain

$$\frac{1}{\pi\sqrt{2a}} G_3(0) \log x < \infty , \quad -\frac{2}{\pi\sqrt{2a}} G_3(0) \log s < \infty . \qquad (50a,b)$$

In the third integral equation (24) the coefficients of the logarithmic terms cancel out. At the end point, we have $x = 0-$ and $s = 0^+$. Hence, from (50) it follows that

$$G_3(0) = 0 . \qquad (51)$$

Therefore, the characteristic equation (46) found by assuming that $\phi_3(0) \neq 0$ (which means that $f_3(0) \neq 0$ or $G_3(0) \neq 0$) would not be valid. Going back now to the system of equations (42-44), if we let $\phi_3(0) = 0$, and assume that $\phi_1(0) \neq 0$ and $\phi_2(0) \neq 0$ (42) and (43) gives

$$\frac{1}{\sin\pi\beta} (1 - \cos\pi\beta - 4\beta + 2\beta^2) = 0 , \qquad (52)$$

and from (44) we obtain

$$\phi_1(0) = \frac{\pi}{2} \phi_2(0) \ . \tag{53}$$

It should be pointed out that (52) is the characteristic equation corresponding to a 90-degree elastic wedge for which the tractions in the neighborhood of the apex are zero. In the problem under consideration, since $\sigma_{yy}(x,0) = 0$ and $\phi_3(0) = 0$ implies that $\sigma_{xy}(-0,0) = 0$, this result is expected[*]. The relation (53) indicates that even though bounded and nonzero, at $(x=0, y=0)$ the displacement derivatives $\partial(u_2^+ - u_2^-)/\partial y$ and $\partial(v_2^+ - v_2^-)/\partial y$ are not independent. In passing one may also remark that at $y=0$, if one forces the crack to close (i.e., if $\phi_1(0) = 0$ and $\phi_2(0) = 0$) and lets $\phi_3(0) \neq 0$, from (44) one may easily recover the standard characteristic equation, namely $\cot\pi\beta = 0$.

6. Symmetric Cover Plates.

· The formulation of the stiffener-crack problem described in the previous sections may be applied to a cracked half plane containing any number of stiffeners without any difficulty. In particular, the problem is considerably simplified if there are two identical cover plates located symmetrically with respect to the $x=0$ plane and if the crack is oriented along the plane of symmetry. In this case, $f_2(t) = 0$ and the system of integral equations (23-25) reduces to

$$\frac{2\mu_2}{\pi(1+\kappa_2)} \int_c^d \left[-\frac{1}{t-s} - \frac{1}{t+s} - \frac{2t}{(t+s)^2} + \frac{4t^2}{(t+s)^3} \right] f_1(t)dt$$

---

[*] It should be emphasized that the absence of stress singularity at the apex of a 90-degree elastic wedge stiffened on one side is due to the membrane assumption made for the stiffener. If the stiffener has a finite thickness, then the apex is a point of stress singularity and the asymptotic behavior of the stress state around this point is similar to that of two bonded dissimilar 90-degree elastic wedges (see, for example, [5]).

$$+ \frac{4}{\pi} \int_{-2a}^{-b} \frac{t^3}{(t^2+s^2)^2} f_3(t)dt = -p_0 \ , \ (c < s < d) \ , \tag{54}$$

$$\frac{2\mu_2}{\pi(1+\kappa_2)} \int_c^d [- \frac{t}{t^2+x^2} + \frac{t(t^2-3x^2)}{(t^2+x^2)^2}] f_1(t)dt + \frac{1}{\pi} \int_{-2a}^{-b} (\frac{1}{t-x} + \frac{1}{t+x}) f_3(t)dt$$

$$- \frac{1+\kappa_1}{2h\mu_1} \frac{\mu_2}{1+\kappa_2} \int_{-2a}^x f_3(t)dt = - \frac{p_0}{2} \ , \ (-2a < x < -b) \ , \tag{55}$$

where it is assumed that the stiffeners are located on $(-2a < x < -b, y=0)$ and $(b < x < 2a, y=0)$, and the crack on $(x=0, -d < y < -c)$. The equilibrium and the single-valuedness conditions under which (54) and (55) must be solved are

$$\int_c^d f_1(t)dt = 0 \ , \ \int_{-2a}^{-b} f_3(t)dt = 0 \ . \tag{56a,b}$$

In this problem, too, the interesting case is that of $c=0$, $b=0$ corresponding to the crack initiation and growth from a broken cover plate. In the case of a single cover plate $-2a < x < 2a$, in the absence of any cracks in the elastic half plane, the maximum tensile stress σ_{xx} in the cover plate would be at $x=0$. If the cover plate fails at this point, then the problem reduces to that discussed in [3], where it was shown that the stress state (in the half plane) at the point $(x=0, y=0)$ has a strong singularity. This would greatly enhance the possibility of crack initiation in the elastic half plane around this point. For $b=0$ and $c=0$ the asymptotic behavior of the solution of (54) and (55) may again be examined by defining f_1 and f_3 as in (36) and (38) and by using the function-theoretic method described in the previous section. In this case, the characteristic equations are found to be

$$\frac{\phi_1(d)}{d^\beta} \cot\pi\omega = 0 \; , \quad \frac{\phi_3(-2a)}{(2a)^\beta} \cot\pi\alpha = 0 \; , \tag{57a,b}$$

$$\frac{1}{\sin\pi\beta} \left[(1-\cos\pi\beta-4\beta+2\beta^2) \frac{\phi_1(0)}{d^\omega} + 2(\beta-2)\cos\frac{\pi\beta}{2} \frac{\phi_3(0)}{(2a)^\alpha} \right] = 0 \; , \tag{58}$$

$$\frac{1}{\sin\pi\beta} \left[-2\beta \cos\frac{\pi\beta}{2} \frac{\phi_1(0)}{d^\omega} - (1+\cos\pi\beta) \frac{\phi_3(0)}{(2a)^\alpha} \right] = 0 \; . \tag{59}$$

Equation (57) gives again the standard result $\omega = 1/2$, $\alpha = 1/2$ and the coefficient determinant Δ of (58) and (59) may be shown to be

$$\Delta(\beta) = \frac{\cos^2\pi\beta-1}{\sin^2\pi\beta} \; . \tag{60}$$

It is again seen that $\Delta(\beta) = 0$ has no root (for which $0 < \text{Re}(\beta) < 1$).

If one now assumes that at the end point $t=0$ f_1 and f_2 are bounded and are of the form given by (49a) and (49c), by using the procedure of the previous section, it may be shown that $G_3(0)$ and hence $f_3(0)$ is zero. In the asymptotic relation obtained from the second integral equation, the coefficients of the logarithmic terms cancel out, implying that $\phi_1(0)$ is bounded and (may be) nonzero (see, for example, [9] for details).

7. Results.

The integral equations with a simple Cauchy kernel or with a generalized Cauchy kernel found in the previous sections are solved by using the numerical integration formulas described, for example, in [7]. The stress intensity factors defined by (27-29) for the problem of a uniformly loaded stiffened cracked elastic half plane are given in Tables 1-6. Tables 1 and 2 show the stress intensity factors for

-18-

the interface shear stress at the end points x=0 and x=-2a of the stiffener for the case of an internal crack (c > 0, θ = 0, Figure 1). In Table 1, the length of the crack is fixed and its relative distance to the boundary s_0 = (d+c)/2a is varied. In Table 2, the crack length is varied for a fixed distance. In the tables the dimensionless constant λ^* defined by

$$\lambda^* = \frac{a}{h} \frac{\mu_2(1+\kappa_1)}{\mu_1(1+\kappa_2)} \tag{61}$$

is a measure of the relative stiffness of the cover plate, smaller λ^* corresponding to stiffer cover plates. The tables indicate the expected trends, namely that generally the stress intensity factors increase with increasing cover plate stiffness. Tables 3 and 4 show the corresponding stress intensity factors at the ends of the internal crack which are defined by (27 and 28). It may be seen that the mode II stress intensity factors $k_2(c)$ and $k_2(d)$ are very small in comparison with the mode I values $k_1(c)$ and $k_1(d)$ indicating that a subcritically growing crack generally would remain in the direction approximately perpendicular to the boundary. One may also observe that the mode I values tend to slightly decrease with increasing cover plate stiffness or decreasing λ^*.

Table 5 shows the results for the edge crack (i.e., c=0) in a half plane stiffened by a single cover plate. Note that in this case, $k_2(0)$ for the interface shear is zero. The results are given only for (d/a) $\le$ 1 as they appear to remain relatively constant for (d/a) > 1. This may be seen from Figure 5 giving the mode I stress intensity factor at the crack tip as a function of d/a. The asymptotic value of the stress intensity ratio for (d/a) → ∞ shown in the figure is that of a uniformly loaded unstiffened half plane containing an edge crack. The figure shows that as (d/a) → 0 the stress intensity factor becomes unbounded. This is, of course, due to the fact that in this case, the governing stress field itself is singular (see Figure 3). It may also be seen that as λ^* decreases, the stress intensity factors tend to increase due to the increase in the "stress concentration" around the stiffener.

-19-

The results for two symmetric cover plates are shown in Table 6. In this case, the stress intensity factor for the contact shear $k_2(0)$ and that at the crack tip for mode II $k_2(d)$ are zero. The important stress intensity factor $k_1(d)$ is also given in Figure 6. Again, it may be seen that for $(d/a) > 1$, the effect of the cover plates appears to be negligible (this general result may also be observed from the stress distributions given in Figures 3 and 4). Comparison of the results given in Figures 5 and 6 indicates that the stress intensity factor for the two cover plate case is consistently greater than that for a single cover plate.

References

1. Bufler, H., "Scheibe mit endlicher, elastischer Versteifung", VDI-Forschungsheft 485, 1961.

2. Arutiunian, N. Kh., "Contact Problem for a Half Plane with Elastic Reinforcement", J. Appl. Math. Mech. (PMM), Vol. 32, 1968, pp. 652-665.

3. Erdogan, F., "Analysis of Elastic Cover Plates", Developments in Mechanics, Vol. 6, Proc. 12th Midwestern Mechanics Conference, 1971, pp. 817-830.

4. Hasebe, N., "Uniform Tension of a Semi-Infinite Plate with a Crack at an End of a Stiffened Edge", Ingenieur-Archiv, Vol. 48, 1979, pp. 129-141.

5. Hein, V.L. and Erdogan, F., "Stress Singularities in a Two-Material Wedge", Int. Journal of Fracture Mechanics, Vol. 7, 1971, pp. 317-330.

6. Dundurs, J., "Elastic Interaction of Dislocations with Inhomogeneities", Mathematical Theory of Dislocations, T. Mura, ed., ASME, 1969, pp. 70-115.

7. Erdogan, F., "Mixed Boundary Value Problems in Mechanics", Mechanics Today, S. Nemat-Nasser, ed., Vol. 4, Pergammon Press, Oxford, 1978, pp. 1-86.

8. Muskhelishvili, I.N., Singular Integral Equations, P. Noordhoff N.V.-Groningen-Holland, 1953.

9. Gupta, G.D., and Erdogan, F., "The Problem of Edge Cracks in an Infinite Strip", J. Appl. Mech., Vol. 41, Trans. ASME, 1974, pp. 1001-1006.

Table 1. Variation of the stress intensity factors $k_2(-2a)$ and $k_2(0)$ for the interface shear stress with the crack location, $s_0=(d+c)/(2a)$ - the case of internal crack, $\lambda^*=(a/h)(\mu_2/\mu_1)(1+\kappa_1)/(1+\kappa_2)$, $\ell=(d-c)/(2a) = 1$.

	$k_2(-2a)/p_0\sqrt{a}$			$k_2(0)/p_0\sqrt{a}$		
s_0 \ λ^*	0.2	1	4	0.2	1	4
1.1	0.519	0.406	0.237	-1.074	-0.918	-0.633
1.5	0.605	0.488	0.305	-0.642	-0.521	-0.325
2	0.602	0.494	0.321	-0.546	-0.442	-0.279
3	0.541	0.447	0.296	-0.493	-0.402	-0.260
5	0.487	0.401	0.264	-0.474	-0.389	-0.255

Table 2. Variation of $k_2(-2a)$ and $k_2(0)$ with crack length, $\ell=(d-c)/2a$, $s_0=(d+c)/(2a) = 1$.

	$k_2(-2a)/p_0\sqrt{a}$			$k_2(0)/p_0\sqrt{a}$		
ℓ \ λ^*	0.2	1	4	0.2	1	4
0.1	0.472	0.388	0.254	-0.473	-0.389	-0.255
0.25	0.478	0.391	0.255	-0.486	-0.399	-0.260
0.5	0.496	0.402	0.256	-0.543	-0.445	-0.286
0.75	0.510	0.406	0.248	-0.700	-0.580	-0.375
0.9	0.494	0.387	0.228	-1.015	-0.867	-0.598

Table 3. Variation of the stress intensity factors at the crack tips $s=c$ and $s=d$ with the crack location, $s_0=(c+d)/(2a)$, $\ell=(d-c)/(2a)=1$ (internal crack).

s_0 \ λ^*	$k_1(c)/p_0\sqrt{\ell a}$			$k_2(c)/p_0\sqrt{\ell a}$			$k_1(d)/p_0\sqrt{\ell a}$			$k_2(d)/p_0\sqrt{\ell a}$		
	0.2	1	4	0.2	1	4	0.2	1	4	0.2	1	4
1.1	1.535	1.550	1.592	-0.077	-0.045	-0.001	1.092	1.116	1.155	0.075	0.062	0.040
1.5	1.055	1.088	1.140	0.042	0.035	0.021	1.034	1.048	1.071	0.052	0.040	0.022
2.0	1.010	1.030	1.059	0.051	0.039	0.024	1.023	1.030	1.041	0.035	0.026	0.014
3.0	1.011	1.017	1.025	0.029	0.022	0.011	1.015	1.017	1.021	0.016	0.012	0.006
5.0	1.008	1.009	1.010	0.008	0.006	0.003	1.008	1.008	1.009	0.005	0.004	0.002

Table 4. Variation of the stress intensity factors at the crack tips with the crack length, $\ell=(d-c)/(2a)$, $s_0=(c+d)/(2a)=1$ (internal crack).

ℓ \ λ^*	$k_1(c)/p_0\sqrt{\ell a}$			$k_2(c)/p_0\sqrt{\ell a}$			$k_1(d)/p_0\sqrt{\ell a}$			$k_2(d)/p_0\sqrt{\ell a}$		
	0.2	1	4	0.2	1	4	0.2	1	4	0.2	1	4
0.1	0.913	0.935	0.967	0.035	0.027	0.015	0.919	0.940	0.970	0.039	0.030	0.016
0.25	0.919	0.943	0.979	0.033	0.026	0.014	0.932	0.952	0.982	0.042	0.032	0.017
0.5	0.965	0.993	1.037	0.023	0.020	0.014	0.966	0.987	1.018	0.050	0.039	0.021
0.75	1.130	1.160	1.212	-0.008	0.001	0.010	1.021	1.044	1.081	0.062	0.050	0.030
0.9	1.500	1.512	1.549	-0.083	-0.050	-0.004	1.080	1.105	1.145	0.073	0.061	0.040

Table 5. Stress intensity factors $k_2(-2a)$, $k_1(d)$, and $k_2(d)$ for the case of a single stiffener and an edge crack (c=0) (see insert in Figure 5).

	$k_2(-2a)/p_0\sqrt{a}$			$k_1(d)/p_0\sqrt{d/2}$			$k_2(d)/p_0\sqrt{d/2}$		
d/a $\diagdown$ λ^*	0.2	1	10	0.2	1	10	0.2	1	10
0.1	0.441	0.369	0.169	2.670	2.434	1.838	-0.380	-0.300	-0.095
0.25	0.393	0.335	0.161	1.959	1.877	1.667	-0.184	-0.143	-0.039
0.5	0.308	0.269	0.138	1.687	1.667	1.606	-0.071	-0.055	-0.015
1	0.152	0.138	0.081	1.591	1.589	1.586	-0.010	-0.008	-0.002

Table 6. Stress intensity factors $k_2(-2a)$ and $k_1(d)$ for two symmetric stiffeners and an edge crack (c=0) (see insert in Figure 6).

	$k_2(-2a)/p_0\sqrt{a}$			$k_1(d)/p_0\sqrt{d/2}$		
d/a $\diagdown$ λ^*	0.2	1	10	0.2	1	10
0.1	0.469	0.386	0.171	4.014	3.443	2.110
0.25	0.402	0.341	0.162	2.351	2.183	1.753
0.5	0.308	0.269	0.139	1.792	1.750	1.632
1	0.152	0.138	0.081	1.601	1.597	1.587

The functions K_{ij} appearing in equations (1):

$$K_{11} = \frac{y+y_1}{(y+y_1)^2+(x-x_1)^2} - \frac{y-y_1}{(y-y_1)^2+(x-x_1)^2} + \frac{2(x-x_1)^2(y+y_1)}{[(y+y_1)^2+(x-x_1)^2]^2}$$

$$- \frac{2(x-x_1)^2(y-y_1)}{[(y-y_1)^2+(x-x_1)^2]^2} - 2y_1\Big[\frac{6(x-x_1)^2(y+y_1)^2+2y_1(y+y_1)^3-6(x-x_1)^2y_1(y+y_1)-2(x-x_1)^4}{[(y+y_1)^2+(x-x_1)^2]^3}$$

$$+ \frac{(x-x_1)^2-(y+y_1)^2}{[(y+y_1)^2+(x-x_1)^2]^2}\Big] \, ,$$

$$K_{12} = (x-x_1)\Big\{ \frac{(x-x_1)^2-(y-y_1)^2}{[(y-y_1)^2+(x-x_1)^2]^2} - \frac{(x-x_1)^2-(y+y_1)^2}{[(y+y_1)^2+(x-x_1)^2]^2}$$

$$- 4y_1 \frac{y[(y+y_1)^2-(x-x_1)^2] + 2(y+y_1)[(x-x_1)^2-(y+y_1)^2+2y_1(y+y_1)]}{[(y+y_1)^2+(x-x_1)^2]^3}\Big\} \, ,$$

$$K_{21} = - \frac{x-x_1}{(y+y_1)^2+(x-x_1)^2} + \frac{x-x_1}{(y-y_1)^2+(x-x_1)^2} - \frac{2(x-x_1)(y-y_1)^2}{[(y-y_1)^2+(x-x_1)^2]^2}$$

$$+ \frac{2(x-x_1)[(y+y_1)^2-2y_1(y+y_1)]}{[(y+y_1)^2+(x-x_1)^2]^2}$$

$$+ 4y_1 \frac{(x-x_1)^3(2y+y_1)+(x-x_1)[3y_1(y+y_1)^2-2(y+y_1)^3]}{[(y+y_1)^2+(x-x_1)^2]^3} \, ,$$

$$K_{22} = -\frac{(y-y_1)[(y-y_1)^2-(x-x_1)^2]}{[(y-y_1)^2+(x-x_1)^2]^2} + \frac{(y+y_1)[(y+y_1)^2-(x-x_1)^2]}{[(y+y_1)^2+(x-x_1)^2]^2}$$

$$-\frac{2y_1}{[(y+y_1)^2+(x-x_1)^2]^3}\{4(x-x_1)^2[(y+y_1)^2-(x-x_1)^2-2y_1(y+y_1)]$$

$$+[(y+y_1)^2+(x-x_1)^2][3(x-x_1)^2-(y+y_1)^2+2y_1(y+y_1)]\} \; ,$$

$$K_{31} = -\frac{(y-y_1)[(y-y_1)^2-(x-x_1)^2]}{[(y-y_1)^2+(x-x_1)^2]^2} + \frac{(y+y_1)[(y+y_1)^2-(x-x_1)^2]}{[(y+y_1)^2+(x-x_1)^2]^2}$$

$$-\frac{2y_1[(y+y_1)^2-(x-x_1)^2]}{[(y+y_1)^2+(x-x_1)^2]^2} - \frac{4yy_1(y+y_1)[(y+y_1)^2-3(x-x_1)^2]}{[(y+y_1)^2+(x-x_1)^2]^3} \; ,$$

$$K_{32} = \frac{x-x_1}{(y-y_1)^2+(x-x_1)^2} - \frac{x-x_1}{(y+y_1)^2+(x-x_1)^2} + \frac{2(x-x_1)(y-y_1)^2}{[(y-y_1)^2+(x-x_1)^2]^2}$$

$$-\frac{2(x-x_1)(y+y_1)^2}{[(y+y_1)^2+(x-x_1)^2]^2} - \frac{4(x-x_1)yy_1[3(y+y_1)^2-(x-x_1)^2]}{[(y+y_1)^2+(x-x_1)^2]^3} \; .$$

APPENDIX B

The kernels k_{ij} appearing in equations (12):

$$k_{11}(s,t) = \frac{2\mu_2}{\pi(\kappa_2+1)} \left\{ \frac{-\cos\theta}{t-s} + [2(t-s)\sin^2\theta\cos\theta - (t+s)\cos^3\theta]R^{-2} \right.$$

$$+ [(t-s)(5t^2-s^2)\sin^2\theta\cos^3\theta-2t(t+s)^2\cos^5\theta - (t-s)^3\cos\theta\sin^4\theta]R^{-4}$$

$$+ [4t^2(t+s)^3\cos^7\theta + 8t^2(t+s)(4ts-t^2-s^2)\sin^2\theta\cos^5\theta$$

$$\left. -12t^2(t-s)^2(t+s)\sin^4\theta\cos^3\theta]R^{-6}\right\},$$

$$k_{12}(s,t) = \frac{2\mu_2}{\pi(\kappa_2+1)} \left\{ \frac{-\sin\theta}{t-s} + (t-s)\sin^3\theta R^{-2} \right.$$

$$+ \sin\theta\cos^4\theta[(t+s)(t^2-s^2-8ts) + 4ts(t-s)]R^{-4}$$

$$+ \sin^3\theta\cos^2\theta(t-s)(17t^2+s^2-10ts)R^{-4}$$

$$+ [8\sin\theta\cos^6\theta t(t-s)^2(t+s)^2 - \sin^5\theta\cos^2\theta 4t(t-s)^3(4t-3s)$$

$$\left. + 4\sin^3\theta\cos^4\theta t(t^2-s^2)(s^2-2t^2+7ts)]R^{-6}\right\},$$

$$k_{13}(s,x_0) = - \frac{2}{\pi}\left\{[(s\sin\theta-x_0)^3\cos^2\theta + s^2\sin^2\theta\cos^2\theta(s\sin\theta-x_0)\right.$$

$$\left. -2\sin\theta\cos^2\theta s(s\sin\theta-x_0)^2][s^2\cos^2\theta+(s\sin\theta-x_0)^2]^{-2}\right\},$$

$$k_{21}(s,t) = \frac{2\mu_2}{\pi(\kappa_2+1)} \left\{ -\frac{\sin\theta}{t-s} + [(t-s)(\sin^3\theta-\sin\theta\cos^2\theta)-(t+s)\sin\theta\cos^2\theta]R^{-2} \right.$$

$$+ [(t+s)(2ts-s^2-5t^2)\sin\theta\cos^4\theta + (t-s)^2(3t-s)\sin^3\theta\cos^2\theta]R^{-4}$$

$$+ [4t(t+s)^2(t-s)(2t-s)\sin\theta\cos^6\theta + 8ts(t-s)(3t^2-s^2)\sin^3\theta\cos^4\theta$$

$$\left. -4t(t-s)^3(2t+s)\sin^5\theta\cos^2\theta]R^{-6} \right\} ,$$

$$k_{22}(s,t) = \frac{2\mu_2}{\pi(1+\kappa_2)} \left\{ \frac{\cos\theta}{t-s} - (t-s)\sin^2\theta\cos\theta R^{-2} + (8t(t-s)^2\cos\theta\sin^4\theta \right.$$

$$+ \cos^3\theta\sin^2\theta[(t+s)(t^2-s^2-4ts) - 2(t-s)(5t^2+s^2-2ts)]$$

$$+ (t+s)(s^2-t^2+4ts)\cos^5\theta)R^{-4} + [4t(t-s)(t+s)(4t^2-3s^2$$

$$- 7ts)\sin^2\theta\cos^5\theta + 4t(t-s)^3(2t-s)\sin^4\theta\cos^3\theta$$

$$\left. - 8t(t-s)^4\sin^6\theta\cos\theta]R^{-6} \right\} ,$$

$$k_{23}(s,x_0) = - \frac{2}{\pi} [s^2\cos^2\theta + (s\sin\theta-x_0)^2]^{-2}[(s\sin\theta-x_0)^3\sin\theta\cos\theta$$

$$- s^2(s\sin\theta-x_0)\cos^3\theta\sin\theta - s(s\sin\theta-x_0)^2(\sin^2\theta-\cos^2\theta)\cos\theta],$$

$$R^2 = (t+s)^2\cos^2\theta + (t-s)^2\sin^2\theta .$$

$$k_{31}(x,t) = \frac{t \cos\theta}{2\pi} \{-T^{-2} + [t^2\cos^2\theta - 3(x-t\sin\theta)^2]T^{-4}\},$$

$$k_{32}(x,t) = -\frac{2}{\pi} t^2(x-t\sin\theta)\cos^2\theta \, T^{-4} ,$$

$$k_{33}(x,x_0) = \frac{1+\kappa_2}{4\mu_2} \frac{1}{\pi} \frac{1}{x_0-x} - \frac{1+\kappa_1}{8h\mu_1} H(x-x_0) ,$$

$$T^2 = t^2\cos^2\theta + (x-t\sin\theta)^2 ,$$

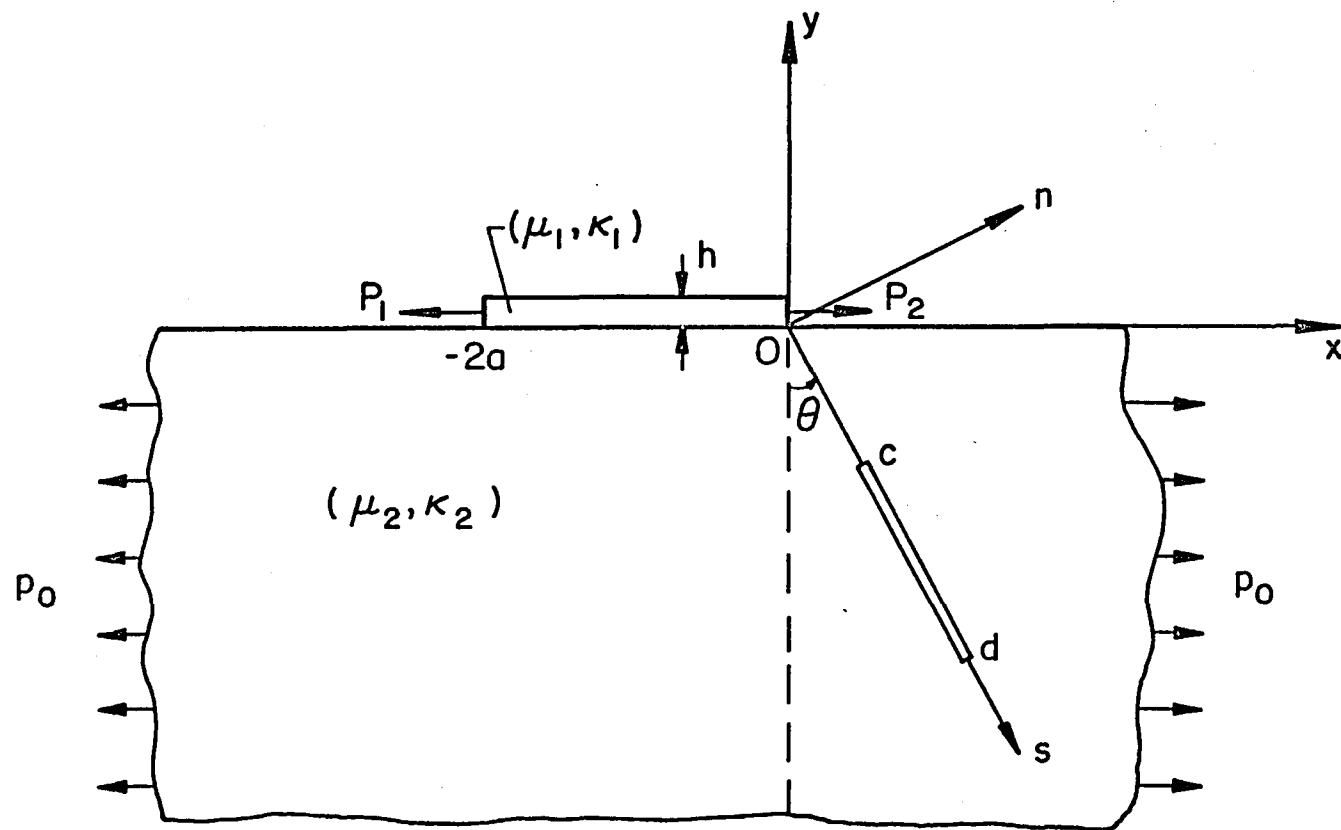$$H(x-x_0) = \begin{cases} 1 , & x > x_0 \\ 0 , & x < x_0 \end{cases} .$$

Fig. 1   Geometry of the stiffened elastic half plane containing
a crack.
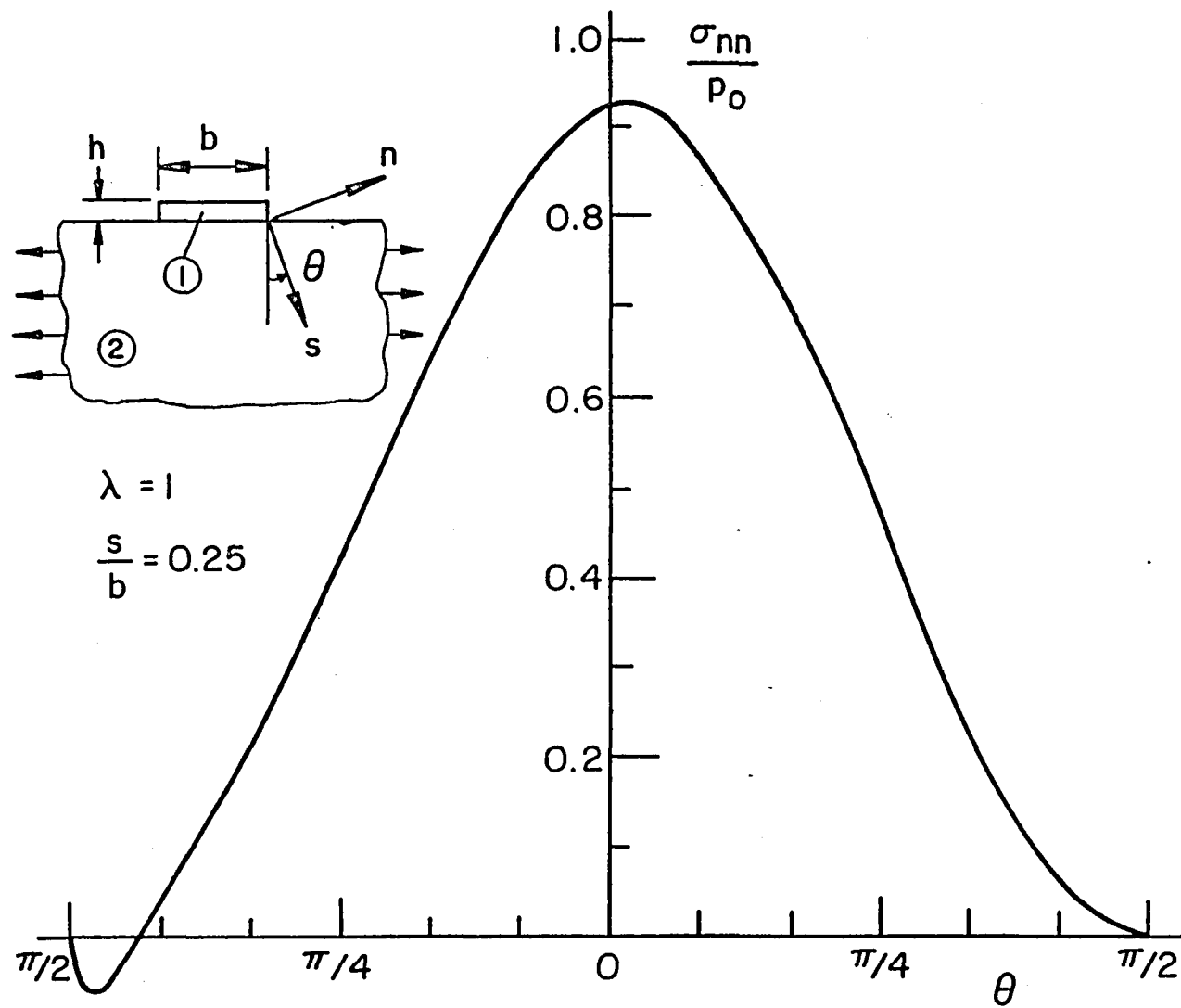
Fig. 2   Angular distribution of the cleavage stress σ_{nn} in the half
plane around the end point of the stiffener.
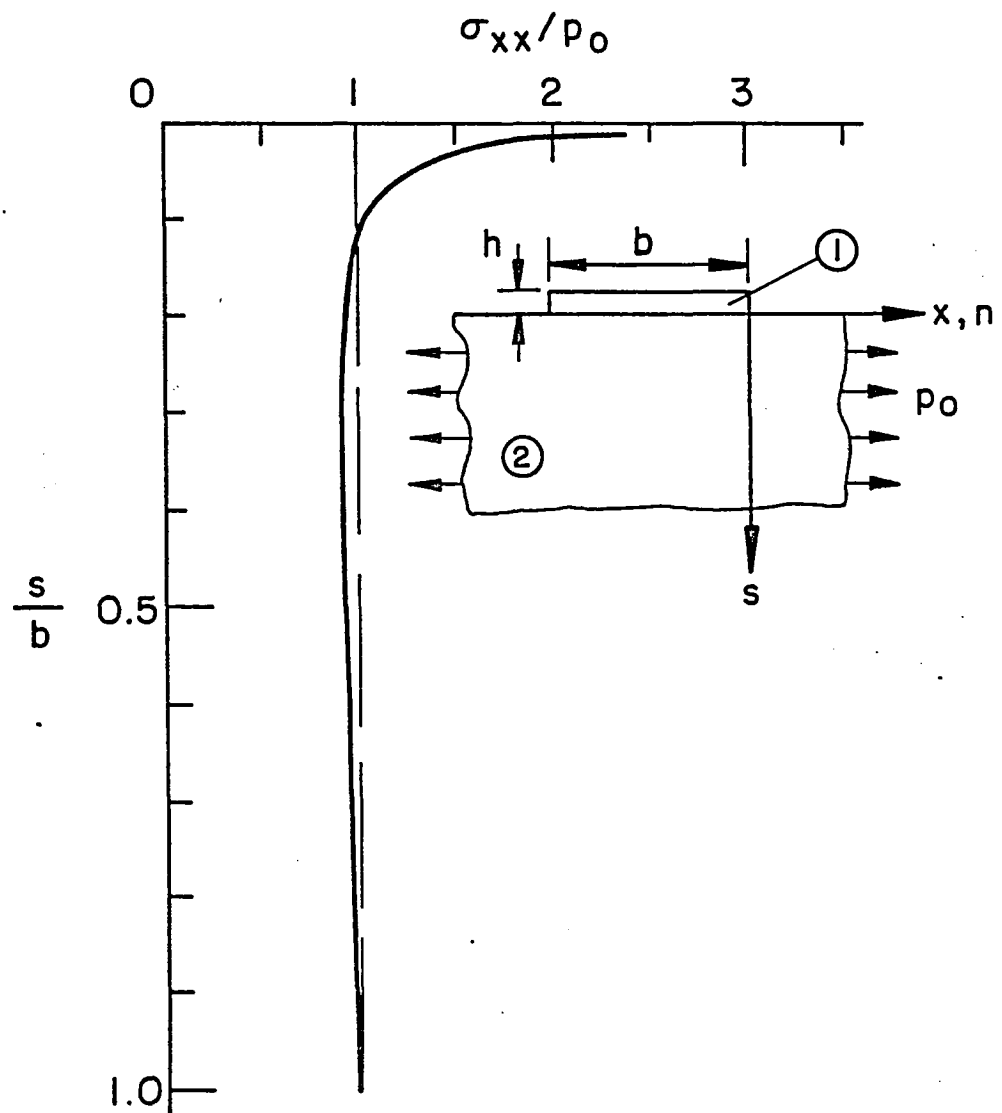
Fig. 3   Variation of the cleavage stress σ_{nn} with the radial distance from an end point of the stiffener for $\theta=0$.
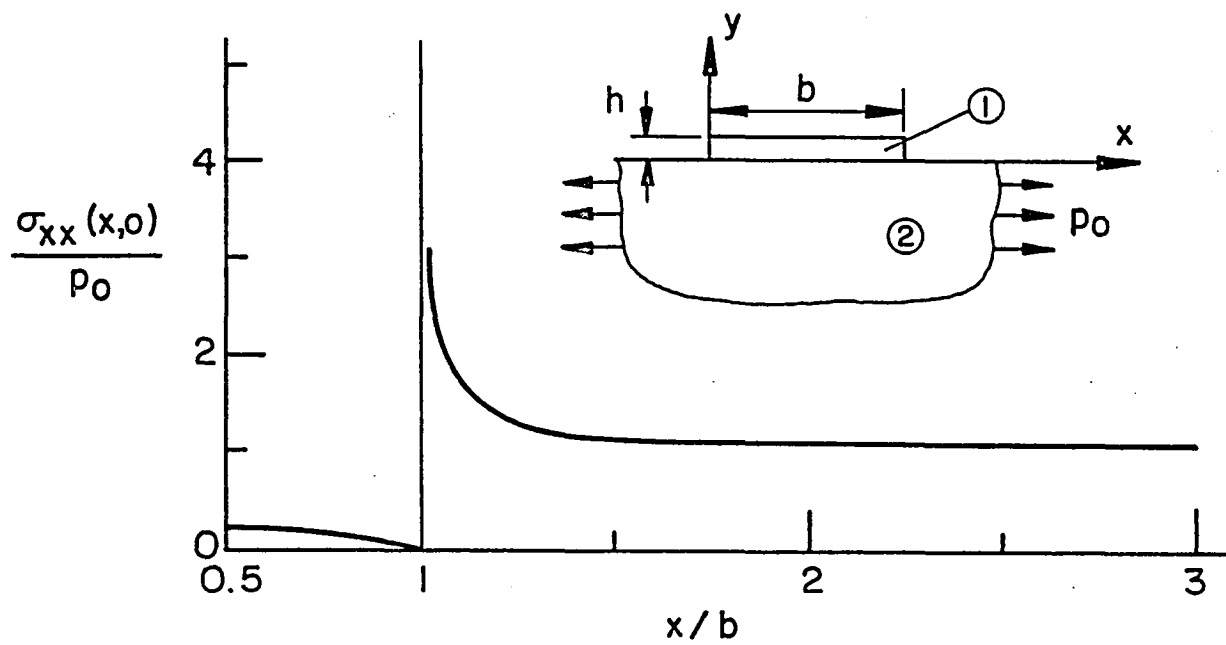
Fig. 4   Variation of the normal stress σ_{xx} on the surface of the stiffened half plane.
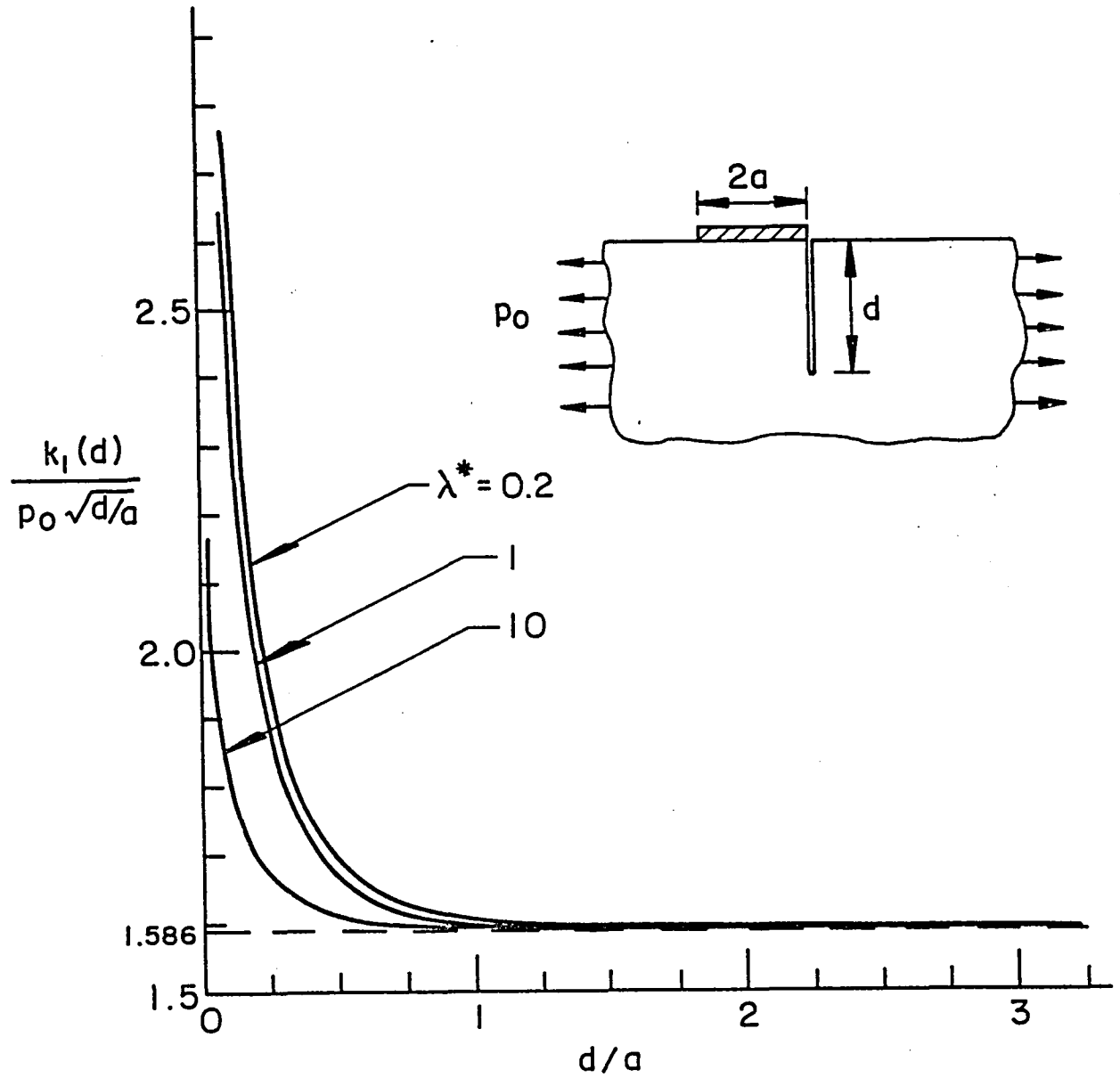
Fig. 5 Variation of the mode I crack tip stress intensity factor with the crack length for various stiffness parameters $\lambda^* = [a\mu_2(1+\kappa_1)]/[h\mu_1(1+\kappa_2)]$ in a half plane containing an edge crack and a single stiffener.
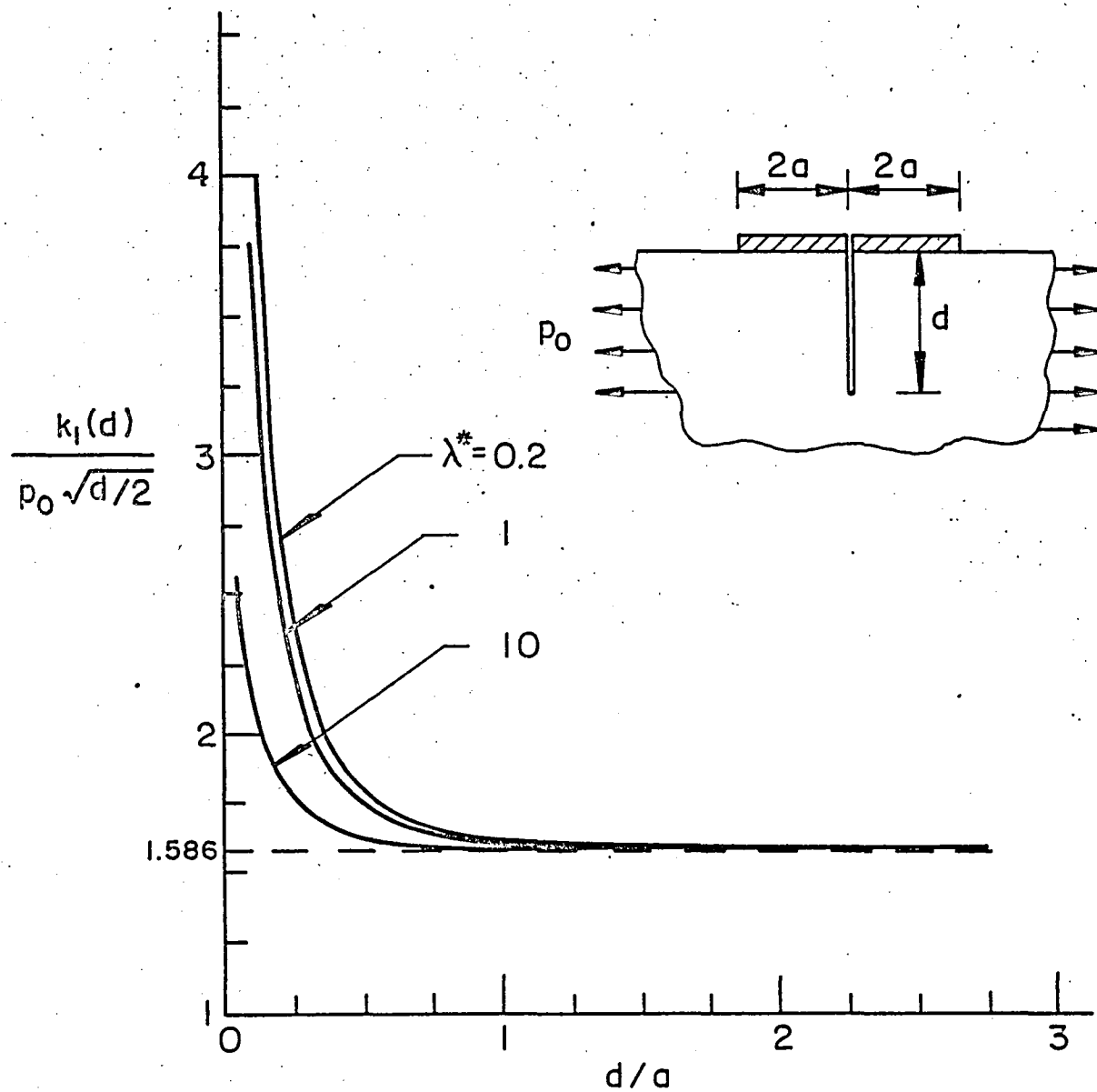
Fig. 6 Variation of the mode I crack tip stress intensity factor with the crack length in a half plane containing an edge crack and stiffened by two symmetric cover plates. $\lambda^* = [a\mu_2(1+\kappa_1)]/[h\mu_1(1+\kappa_2)]$.